

Interfacing Statistical Turbulence Closures with Large-Eddy Simulation

Paul Batten,* Uriel Goldberg,† and Sukumar Chakravarthy‡
Metacomp Technologies, Inc., Agoura Hills, California 91301

Progress toward a general purpose hybrid Reynolds-averaged Navier–Stokes (RANS)/large-eddy simulation (LES) framework is described, in which large-scale, statistically represented turbulence kinetic energy is converted automatically into resolved-scale velocity fluctuations wherever the local mesh resolution is sufficient to support them. Existing hybrid RANS/LES approaches alter the nature of the local partial differential equations according to the local mesh resolution, but they do not alter the nature of the data on which these equations operate. The implications of this are discussed. Subsequently, a simple mechanism is introduced to transfer statistical kinetic energy into resolved-scale fluctuations in a manner that preserves a given set of space/time correlations and set of second moments. This process, which can appropriately be termed Large-Eddy STimulation (LEST), generates the large-scale eddies needed to form the unsteady boundary conditions at RANS interfaces to LES regions, into which turbulence energy can be deposited either through mean convection or through turbulent transport. The proposed approach is designed to work on general meshes with arbitrary clusterings and does not require the user to specify internal boundary surfaces separating RANS and LES regions. Results on a plane channel flow show that the approach helps to preserve the shear stress across regions where turbulence is transported by mean convection and also helps to sustain the fluctuations in the outer, unsteady, portion of the boundary layer by reconstructing the resolved-scale energy that is generated in the statistically modeled near-wall layer and transported across the boundary layer via turbulent mixing.

Nomenclature

c^n	= velocity scaling for n th mode, m/s
d_j^n	= wave vector of n th mode
k	= turbulence kinetic energy, m^2/s^2
L	= turbulence length scale ($k^{3/2}/\epsilon$), m
S	= nondimensional strain magnitude
S_{ij}^*	= mean strain tensor, s^{-1}
V	= turbulence velocity scale ($k^{1/2}$), m/s
x_j	= position vector in Cartesian frame
α	= limited numerical scale (LNS) latency parameter
Δ	= LNS filter width, $2 \max[\Delta x, \Delta y, \Delta z, \Delta t \sqrt{(u_i^2)}]$
δ_{ij}	= Kronecker delta
ϵ	= turbulence dissipation rate, m^2/s^3
ϵ_{ijk}	= alternating symbol
μ_t	= turbulence eddy viscosity, $kg/(m \cdot s)$
ρ	= density, kg/m^3
τ	= turbulence timescale (L/V), s
$\bar{\phi}$	= time-average of ϕ
$\tilde{\phi}$	= Favre average of ϕ
Ω	= nondimensional vorticity magnitude
Ω_{ij}^*	= mean vorticity tensor, s^{-1}

I. Introduction

THE need to simulate high-Reynolds-number, unsteady turbulent flows has resulted in a recent surge of interest in hybrid methods that attempt to combine the best features of Reynolds-

averaged Navier–Stokes (RANS) turbulence closures with large-eddy simulation (LES) (for example, see Refs. 1–11). Traditional LES becomes impractical at high Reynolds numbers because of the small size of the boundary-layer eddies responsible for the major portion of the near-wall shear stress. Hybrid methods relax this stringent requirement on spatial and temporal resolution, by allowing certain regions of the time-dependent flowfield to be treated with traditional RANS models. Calculations from a number of research groups, for example, Refs. 2, 4, 6, 10, and 11, have shown that these hybrid methods can produce good results for a class of separated flows in which unsteadiness is strongly self-sustaining and the unsteady effects in the separating boundary layer can be considered negligible. However, existing hybrid models are not well suited to flows involving impingement, thin separation, or indeed any region in which the local mesh undergoes an abrupt, isotropic refinement and where flow instabilities are too weak to initiate the large-scale unsteady motions. The reasons for these potential failure modes are discussed.

This paper then describes an attempt to generalize these hybrid methods to all types of flow and to arbitrary meshes, which can include embedded fine-grid regions. This generalization is achieved by an automatic transfer of statistically represented kinetic energy data into directly resolved fluctuations, in a manner consistent with the length and timescales of the statistical turbulence, the second moments, and the resolvable fraction of the turbulence energy. The latter is reconstructed using a sum of Fourier modes, as proposed by Kraichnan,¹² with a tensor scaling based on the Cholesky decomposition of the local Reynolds-stress tensor; the latter being a simplified form of the tensor scaling proposed by Smirnov et al.¹³ The proposed synthetic reconstruction involves no additional transport equations and requires no additional grid-related storage.

The reported work is still preliminary, but demonstrates, for the first time, hybrid RANS/LES boundary-layer calculations, which involve a constant transfer (and translation) of turbulence kinetic energy between the RANS and LES data. Results on a plane channel flow indicate that the energy transfer approach helps to preserve the total shear stress across regions into which turbulence is transported via mean convection. In addition, the approach helps to sustain the fluctuations in the outer, unsteady, portion of the boundary layer, by reconstructing the resolved-scale energy that is generated

Presented as Paper 2003-0081 at the AIAA 41st Aerospace Sciences Meeting, Reno, NV, 10–13 January 2003; received 1 July 2003; revision received 18 October 2003; accepted for publication 23 October 2003. Copyright © 2003 by Metacomp Technologies, Inc. Published by the American Institute of Aeronautics and Astronautics, Inc., with permission. Copies of this paper may be made for personal or internal use, on condition that the copier pay the \$10.00 per-copy fee to the Copyright Clearance Center, Inc., 222 Rosewood Drive, Danvers, MA 01923; include the code 0001-1452/04 \$10.00 in correspondence with the CCC.

*Senior Scientist.

†Principal Scientist.

‡President.

in the statistically modeled near-wall layer and transported across the boundary layer via turbulent mixing.

II. Limited-Numerical-Scales Framework

The hybrid framework used throughout this paper is the limited-numerical-scales (LNS) approach proposed by Batten et al.^{3,4} This method formed the first commercial implementation of a hybrid RANS/LES approach (in the CFD++ code) and was first presented in a conference paper in January 2000.⁵ Because the LNS method has not been presented previously in a journal paper, the following section provides the full details of the method, as it is currently being used.

LNS was inspired by an earlier suggestion of Speziale,¹ whose original proposal was for a hybrid RANS/LES framework in which the stress tensor $\overline{u'_i u'_j}^M$ provided by a (conventional RANS) Reynolds-stress transport model would be damped via

$$\overline{u'_i u'_j} = \alpha \overline{u'_i u'_j}^M \quad (1)$$

in which

$$\alpha = [1 - \exp(-\beta L^\Delta / L^k)]^n \quad (2)$$

where β and n are some (unspecified) parameters, L^Δ is some representative mesh spacing, and L^k is the Kolmogorov length scale

$$L^k = \nu^{3/4} / \bar{\epsilon}^{1/4} \quad (3)$$

The superscript M , denotes values computed using conventional RANS equations. After the scaling in Eq. (1), regular RANS stress levels are recovered whenever L^Δ is much larger than L^k , whereas the subgrid stresses vanish completely as $L^\Delta \rightarrow 0$.

Unfortunately, the parameters β , n in Eq. (2), and the definition of the model equations used to derive the undamped Reynolds stresses were never completely specified by Speziale.¹ There is a wide choice of β and n that would satisfy the two [RANS and direct numerical simulation (DNS)] limits, and not all such choices guarantee that a suitable subgrid-scale (LES) model will be recovered in between.

In the LNS approach,³ the definition of α is determined from the observation that in the commonly used isotropic eddy-viscosity framework the only relevant parameter is the shear stress aligned in an axis parallel to that of the mean shear strain. In Boussinesq models, such as k - ϵ closures or Smagorinsky-type¹⁴ subgrid models, this is typically the only quantity used in the model calibration. LNS therefore redefines the latency factor α using the following ratio of effective-viscosity norms:

$$\alpha = \frac{\min[(f_\mu L \cdot V)_{\text{LES}}, (f_\mu L \cdot V)_{\text{RANS}}]}{(f_\mu L \cdot V)_{\text{RANS}}} \quad (4)$$

The $(f_\mu L \cdot V)_{\text{LES}}$ and $(f_\mu L \cdot V)_{\text{RANS}}$ products denote norms for the effective viscosity arising from the component LES and RANS models, respectively. If consistent models are assumed for both LES and RANS stress tensors, then the preceding latency factor simply selects the shear stress of minimum magnitude.

In current LNS computations, the conventional Smagorinsky approach¹⁴ has been used as the underlying subgrid scale model:

$$\mu_t = C_s (L_i^\Delta)^2 \sqrt{S_{kl}^* S_{kl}^*} / 2 \quad (5)$$

in which C_s is the Smagorinsky coefficient, here taken as 0.05. The parameter L^Δ defines a filter length, which allows the approach to distinguish between unresolvable and resolvable (or at least potentially resolvable) scales of motion. Because the orientation of local flow structures is not, in general, known in advance, a safe requirement is to choose the smallest wavelength that can be supported at any orientation to the local mesh. This leads us to the following measure for the local Nyquist grid wavelength:

$$L_i^\Delta = 4 \max_{k=0 \dots n} (|r_c - r_k|) \quad (6)$$

where n is the number of faces forming cell i , r_c is the centroid of cell i , and r_k is the midpoint of face k . On a structured Cartesian

mesh, this is equivalent to

$$L^\Delta = 2 \max[\Delta x, \Delta y, \Delta z] \quad (7)$$

with the additional factor of two (which is often absorbed into the Smagorinsky constant) accounting for the wavelength corresponding to the Nyquist frequency of the grid.

One can also insist that the time step be small enough to accurately resolve the convective transport of any grid-supportable structures. Thus, the Courant condition based on the local fluid velocity (which defines a basic condition for accuracy in nonlinear flow problems) can be used to provide an additional safety factor in the local length-scale definition. For example, the following extension was proposed by Batten et al.⁴:

$$L^\Delta = 2 \max \left[\Delta x, \Delta y, \Delta z, \sqrt{(u_i^2) \Delta t} \right] \quad (8)$$

where u_i is the local fluid velocity, relative to the mesh. This ensures that, irrespective of the local spatial resolution, the RANS solution is recovered when Δt becomes large. This additional constraint is important in regions of abrupt near-surface mesh clustering, where the temporal resolution would not permit those very fine scale structures to be predicted accurately. (These structures would be on the order of the smallest boundary-layer spacing in all directions, whereas the global time step is typically set to match the larger cell spacings away from the immediate near-wall region.)

The Smagorinsky subgrid-scale (SGS) model requires some form of near-wall damping because, for any finite mesh spacing L^Δ , the nonvanishing strain rate would otherwise imply a nonvanishing turbulent shear stress at the wall. In conjunction with the Smagorinsky model, it has been common practice to employ ad hoc damping functions based on distance to the wall. In the present LNS implementation, a single low-Reynolds-number damping function f_μ is shared by both RANS and LES component models. The use of a single f_μ function simplifies the definition of α :

$$\alpha = \frac{\min[(L \cdot V)_{\text{LES}}, (L \cdot V)_{\text{RANS}}]}{(L \cdot V)_{\text{RANS}}} \quad (9)$$

Using this definition of α in conjunction with Eq. (1), the governing equations behave as RANS if $\alpha = 1$, or LES if $\alpha < 1$. When fine-grid regions are encountered by the LNS method, the scaling of the predicted Reynolds-stress tensor by α causes the effective viscosity to be instantly reduced to the levels implied by the underlying LES subgrid model, with the local flow turbulence also experiencing a decreased rate of production because of the reduced magnitude of the stress-tensor components.

The energy fraction αk is interpreted as unresolvable subgrid turbulence kinetic energy, which can only ever be modeled. The $(1 - \alpha)k$ component is interpreted as resolvable turbulence kinetic energy, which could be represented directly on the local mesh (see Fig. 1). In LNS, the sum total of statistically represented turbulence energy $k(\text{LNS})$ does not have the same meaning as $k(\text{RANS})$ in a traditional RANS closure. In general, $k(\text{LNS}) \leq k(\text{RANS})$.

Similarly, the quantity $\alpha \epsilon$ is interpreted as the dissipation that applies to the unresolvable scales and the quantity $(1 - \alpha)\epsilon$ is

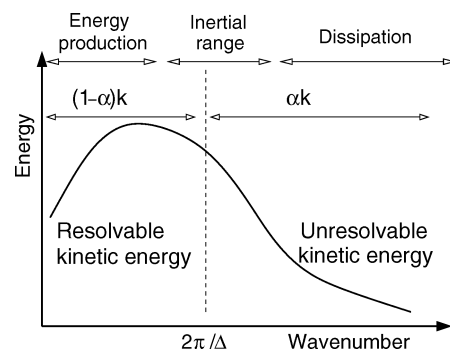


Fig. 1 Turbulence energy spectrum partitioned into resolvable and unresolvable wavelengths.

interpreted as the dissipation or transfer rate, which applies to the resolvable scales. For a linear, Boussinesq closure, these partitions on k and ϵ imply $\mu_t = \alpha \mu_t^M$, that is, that the eddy viscosity from a conventional RANS model is simply scaled by α .

In the present work, the LNS model equations for the unresolved stresses are based on a nonlinear $k - \epsilon$ closure (see Goldberg et al.¹⁵ and references cited therein), in which the Reynolds-stress tensor is defined via a tensorial expansion, cubic in the mean strain and vorticity tensors. Although there is no specific requirement on the baseline RANS model within LNS, the cubic model used here helps ensure realizability (a property that is required for the synthetic reconstruction in Sec. III) and has some theoretical advantages in situations where the underlying RANS model is used to predict the onset of the primary separation. The same expression for the anisotropy tensor is currently used in both RANS and LES component models. The governing equations are given as

$$\frac{\partial \bar{\rho} \bar{k}}{\partial t} + \frac{\partial \bar{\rho} \bar{u}_i \bar{k}}{\partial x_i} = \frac{\partial}{\partial x_i} \left[\left(\mu + \frac{\mu_t}{\sigma_k} \right) \frac{\partial \bar{k}}{\partial x_i} \right] + P_k - \bar{\rho} \bar{\epsilon} \quad (10)$$

$$\begin{aligned} \frac{\partial \bar{\rho} \bar{\epsilon}}{\partial t} + \frac{\partial \bar{\rho} \bar{u}_i \bar{\epsilon}}{\partial x_i} &= \frac{\partial}{\partial x_i} \left[\left(\mu + \frac{\mu_t}{\sigma_\epsilon} \right) \frac{\partial \bar{\epsilon}}{\partial x_i} \right] \\ &+ (C_{\epsilon 1} P_k - C_{\epsilon 2} \bar{\rho} \bar{\epsilon} + E) T_t^{-1} \end{aligned} \quad (11)$$

In the preceding,

$$\begin{aligned} P_k &= -\bar{\rho} \widetilde{u_i'' u_j''} \frac{\partial \bar{u}_i}{\partial x_j} \\ \bar{\rho} \widetilde{u_i'' u_j''} &= \alpha \bar{\rho} \frac{2}{3} \bar{k} \delta_{ij} - \mu_t S_{ij}^* + c_1 \frac{\mu_t \bar{k}}{\bar{\epsilon}} \left(S_{ik}^* S_{kj}^* - \frac{1}{3} S_{kl}^* S_{kl}^* \delta_{ij} \right) \\ &+ c_2 \frac{\mu_t \bar{k}}{\bar{\epsilon}} \left(\Omega_{ik} S_{kj}^* + \Omega_{jk} S_{ki}^* \right) + c_3 \frac{\mu_t \bar{k}}{\bar{\epsilon}} \left(\Omega_{ik} \Omega_{jk} - \frac{1}{3} \Omega_{lk} \Omega_{lk} \delta_{ij} \right) \\ &+ c_4 \frac{\mu_t \bar{k}^2}{\bar{\epsilon}^2} \left(S_{ki}^* \Omega_{ij} + S_{kj}^* \Omega_{li} \right) S_{kl}^* \\ &+ c_5 \frac{\mu_t \bar{k}^2}{\bar{\epsilon}^2} \left(\Omega_{il} \Omega_{lm} S_{mj}^* + S_{il}^* \Omega_{lm} \Omega_{mj} - \frac{2}{3} S_{lm}^* \Omega_{mn} \Omega_{nl} \delta_{ij} \right) \\ &+ c_6 \frac{\mu_t \bar{k}^2}{\bar{\epsilon}^2} S_{ij}^* S_{kl}^* S_{kl}^* + c_7 \frac{\mu_t \bar{k}^2}{\bar{\epsilon}^2} S_{ij}^* \Omega_{kl} \Omega_{kl} \end{aligned}$$

with

$$\begin{aligned} S_{ij}^* &= \left(\frac{\partial \bar{u}_i}{\partial x_j} + \frac{\partial \bar{u}_j}{\partial x_i} \right) - \frac{2}{3} \frac{\partial \bar{u}_k}{\partial x_k} \delta_{ij} \\ \Omega_{ij} &= \left(\frac{\partial \bar{u}_i}{\partial x_j} - \frac{\partial \bar{u}_j}{\partial x_i} \right) \\ S &= \frac{\bar{k}}{\bar{\epsilon}} \sqrt{\frac{1}{2} S_{ij}^* S_{ij}^*}, \quad \Omega = \frac{\bar{k}}{\bar{\epsilon}} \sqrt{\frac{1}{2} \Omega_{ij} \Omega_{ij}} \end{aligned}$$

A realizable turbulence timescale is defined as

$$T_t = (\bar{k}/\bar{\epsilon}) \max\{1, \xi^{-1}\}$$

where $\xi = \sqrt{(R_t)/C_\tau}$, with $R_t = \bar{k}^2/(\nu \bar{\epsilon})$ and $C_\tau = \sqrt{2}$. The eddy viscosity is defined as

$$\mu_t = \alpha C_\mu f_\mu \bar{\rho} \bar{k}^2 / \bar{\epsilon} \quad (12)$$

with

$$\begin{aligned} C_\mu &= \frac{2/3}{A_1 + S + 0.9\Omega} \\ c_1 &= \frac{3/4}{(1000 + S^3)C_\mu}, \quad c_2 = \frac{15/4}{(1000 + S^3)C_\mu} \end{aligned}$$

$$c_3 = \frac{-19/4}{(1000 + S^3)C_\mu}, \quad c_4 = -10C_\mu^2, \quad c_5 = 0$$

$$c_6 = -2C_\mu^2, \quad c_7 = -c_6$$

$$f_\mu = \frac{1 - e^{-A_\mu R_t}}{1 - e^{-\sqrt{R_t}}} \max \left\{ 1, \frac{1}{\xi} \right\}$$

$$E = A_{E_\tau} \bar{\rho} \max \left[\bar{k}^{\frac{1}{2}}, (\nu \bar{\epsilon})^{\frac{1}{4}} \right] \sqrt{\bar{\epsilon} T_t} \Psi_\tau$$

$$\Psi_\tau = \max \left\{ \frac{\partial \bar{k}}{\partial x_j} \frac{\partial \tau}{\partial x_j}, 0 \right\}, \quad \tau = \frac{\bar{k}}{\bar{\epsilon}}$$

From Eq. (9), the latency parameter α is defined for the current choice of RANS and LES component models as

$$\alpha = \min \left\{ \frac{C_s (L_i^\Delta)^2 \sqrt{S_{kl}^* S_{kl}^* / 2}}{C_\mu \bar{k}^2 / \bar{\epsilon} + \delta}, 1 \right\} \quad (13)$$

with δ some small parameter, $\mathcal{O}(10^{-20})$, to allow $\alpha \rightarrow 1$ without singularities in low-Reynolds-number regions. The remaining model constants are

$$\begin{aligned} A_1 &= 1.25, & C_{\epsilon 1} &= 1.44, & C_{\epsilon 2} &= 1.92, & \sigma_k &= 1.0 \\ \sigma_\epsilon &= 1.3, & A_\mu &= 0.01, & A_{E_\tau} &= 0.15, & C_s &= 0.05 \end{aligned}$$

The key distinguishing feature of LNS is that it contains no empirical constants beyond those appearing in the baseline RANS and LES models. Thus, the LNS framework is immediately able to exploit improvements in either RANS or LES modeling, by directly inserting any enhanced component model.

III. Large-Scale Energy Transfer Using Synthetic Turbulence

The energy partition in LNS (and, indeed, in any hybrid RANS/LES) is closely reminiscent of that in earlier multiscale turbulence closures, for example, Hanjalic et al.¹⁶ and Schiestel,¹⁷ in which the turbulence energy is split into large- and small-scale components, with separate dissipation or transfer rates applying to each. The multiscale RANS approach recognizes that there can be a significant time lag between turbulence production via mean strain and its eventual dissipation (into thermal energy) at the finest scales. The computed dissipation at the largest scales (the $1 - \alpha$ fraction in Fig. 1) defines the rate of kinetic energy transfer between the large and fine scales. Only the dissipation at the finest scales is able to reduce the total turbulence kinetic energy. Likewise, in hybrid RANS/LES, large-scale energy should not be instantly dissipated to heat simply to satisfy the requirements of a reduced eddy viscosity; however, this error is common practice in many existing hybrid RANS/LES approaches (for example, see Refs. 1–3 and 6–11). Situations in which large-scale, statistically represented data experience a locally refined mesh require that resolved-scale energy be represented as such. Neglecting this fact (by simply dissipating k to reach some target subgrid stress level) results in a bypass of the usual energy cascade, leading to a component laminarization, in which unresolved (modeled) stresses are suppressed, but resolved-scale fluctuations are never initiated. The net result is an underprediction of the total stress levels.

An important distinction between multiscale RANS models and hybrid RANS/LES is the nature of the data within the largest and smallest scales. In hybrid RANS/LES, turbulence energy in the smallest scales is represented statistically, whereas turbulence energy in the larger scales is represented directly in the resolved velocity components. That distinction means that the transfer of data between the two scales is more complex than in the case of multiscale

RANS closures because the transfer process must also involve a translation between the two types of data representation.

Perhaps the most critical issue facing existing hybrid RANS/LES methodologies occurs when a solution involving a RANS-type boundary or shear layer experiences a sudden, isotropic, mesh clustering. Although the model equations can switch to LES, if the data on which the equations operate do not change accordingly, the result will be a nonphysical drop in the time-averaged total stresses. As a result of this obvious failure mode, several practitioners have advocated the use of recycling, in which streamwise periodic boundary conditions are applied locally, using a rescaling to account for any boundary-layer growth (for example, see Fan et al.⁸). Although the recycling approach has been used successfully in previous LES, it faces considerable challenges in more complex geometries. Furthermore, it places an additional burden on the end user (who is required to position the recycling boundaries), and it accounts only for large-scale energy transferred through mean convection. Recycling cannot account for large-scale energy transported through turbulent motion, for example, across a near-wall RANS layer, which is a process typically modeled via diffusive transport. In this paper, we consider an alternative to recycling at RANS/LES interfaces, which is based on the use of a reconstructed, synthetic turbulence field.

There are two important types of interface to be considered. In either case, these could occur with abrupt or gradual changes in mesh resolution. The first case is the transfer into resolved components of large-scale statistical energy, which is transported into finer, isotropic mesh regions via mean or resolved convection. The second case is the transfer from large-scale statistical energy, which is transported via turbulent motions.

The difficulty in interfacing between RANS and LES in hybrid calculations leads to the possibility of two unique failure modes, which we refer to as component laminarizations. On coarser grids, resolved motions might decay too quickly, leaving the RANS model unable to support all stress levels via modeling.¹⁸ Experience suggests that this failure is strongly dependent on several factors, including spatial resolution, temporal resolution, and numerical method. Conversely, on very fine grids the statistically modeled components can vanish too quickly, leaving the LES unable to support all of the stress levels of a full DNS. Because the RANS model generally has no knowledge of the numerics employed, it seems improbable that any given RANS component model will guarantee laminarization at exactly the point at which the LES calculation becomes a full and accurate DNS. This RANS-component laminarization is, however, a serious difficulty only when approaching the DNS limit. Thus, in practical calculations at even modest Reynolds numbers the more likely mode of failure is that of the LES-component laminarization, which could occur either through a gradual dissipation of the resolved structures or following transport into an isotropic, fine-mesh region in which the resolved components were never directly represented in the first place.

Some of the preceding difficulties have been previously highlighted by Baggett¹⁹ and Nikitin et al.¹⁸ In hybrid RANS/LES computations of channel flow, Baggett¹⁹ observed streamwise structures that were approximately three times too large. As a result, Baggett¹⁹ suggested that hybrid RANS/LES might be inappropriate for use with attached boundary layers. Smaller-scale perturbations from the buffer layer appear to play a crucial role in breaking up the larger-scale structures further away from the wall, and representing this effect on coarse meshes presents an interesting modeling challenge. Nikitin et al.¹⁸ noted the LES component laminarization on coarse meshes, caused by a total dissipation of the resolved structures. However, an interesting recent publication by Peltier and Zajaczkowski²⁰ suggests that an ad hoc random forcing can be successfully used to maintain large-scale unsteady motion in the outer portion of the boundary layer, thereby preventing the component laminarization of the LES core region and maintaining the time-averaged turbulence velocity profile. The methodology presented in this paper provides a rational justification for the use of such forcing, based on a spatially and temporally correlated synthetic reconstruction of the statistical turbulence energy, which diffuses across the near-wall RANS layer.

Many approaches have been proposed for generating inflow conditions for an LES. Possibly the simplest approach involves a superposition of white noise on some mean velocity profile. A further elaboration might be a white-noise signal that would reproduce the single-point statistics. However, most previously reported attempts in this direction have failed because of the rapid dissipation of Nyquist-frequency signals by the subgrid treatment. An important requirement in this synthetic reconstruction is for realistic spatial and temporal correlations, which allow the maintenance and/or regeneration of physical turbulent structures. Although a full set of two-point correlations is generally not known, most RANS closures do provide information on turbulence lengthscales and timescales, which the synthetic model should mimic.

An early proposal for the generation of synthetic turbulence was introduced by Kraichnan¹² in his work on diffusion by turbulent velocity fields. Kraichnan's¹² proposal was based on a sum of Fourier modes and was limited to frozen, isotropic turbulence. More recently, Smirnov et al.¹³ proposed the idea of a tensor scaling based on a similarity transformation of the Reynolds-stress tensor that is able to account for turbulence anisotropy—an essential property if the time-averaged shear stress is to be reproduced. The proposal below presents a simplified alternative to the Smirnov et al.¹³ method, which avoids the need to compute similarity transformations:

$$u_k(x_j, t) = a_{ki} \sqrt{\frac{2}{N}} \sum_{n=1}^N [p_i^n \cos(\hat{d}_j^n \hat{x}_j + \omega^n \hat{t}) + q_i^n \sin(\hat{d}_j^n \hat{x}_j + \omega^n \hat{t})]$$

$$\hat{x}_j = \frac{2\pi x_j}{L}, \quad \hat{t} = \frac{2\pi t}{\tau}, \quad \hat{d}_j^n = d_j^n \frac{V}{c^n}, \quad V = \frac{L}{\tau}$$

$$c^n = \sqrt{\frac{3u'_i u'_m d_i^n d_m^n}{2d_k^n d_k^n}}, \quad p_i^n = \epsilon_{ijk} \eta_j^n d_k^n, \quad q_i^n = \epsilon_{ijk} \xi_j^n d_k^n$$

$$\eta_i^n, \xi_i^n = N(0, 1), \quad \omega^n = N(1, 1), \quad d_i^n = N\left(0, \frac{1}{2}\right) \quad (14)$$

In the preceding equations, a_{ij} is the Cholesky decomposition of $u'_i u'_j$ and $N(\phi, \psi)$ implies a normally distributed random variable with mean ϕ and standard deviation ψ . The preceding method is essentially that proposed by Kraichnan,¹² but with the additional tensor scaling, which accounts for the anisotropy. The time and space correlations are represented by scaling the time and distance coordinates by using the local turbulence timescale τ and (anisotropic) velocity scale c^n taken as a tensorially invariant measure in the direction of the modal wave vector d^n . In the long time average, the synthesized time-dependent flowfield will reproduce the imposed length and time correlations and all second moments. This does not suggest that it will match the full set of two-point correlations from DNS data or experiment, but that the second moments and the average length and time correlations from the RANS data will be preserved. Part of our modeling assumption is that these scales are correlated with the target anisotropy, for example, a larger $\overline{u'u'}$ implies a stronger correlation in the x direction. That assumption is regarded as reasonable in the absence of any other information from the RANS model. It is possible, however, that the reproduced length and time correlations can end up smaller than desired if scaling parameters, such as local timescales, velocity scales, and Cholesky-decomposed matrices, undergo significant spatial variations of their own.

The reconstruction procedure requires, as input, the local stress tensor and length scale and timescale of the turbulence, which is information that can be extracted from the available RANS data. Ideally, a Reynolds-stress transport model would provide the most accurate description of the second moments; however, simpler realizable models are sufficient to recover the shear stress, and the cubic k - ϵ model, currently used in LNS, is also capable of representing normal-stress anisotropy. (Note that all elements of the Cholesky decomposition are real if the target stress tensor is realizable.)

Single-equation eddy-viscosity models, such as that used in the original DES proposal,² are not considered here because they provide no general means of estimating k . Additional modeling assumptions or a modified set of DES equations might be used to circumvent these issues, but such an approach is not pursued here.

Because each mode in the preceding Fourier model has an associated wavelength (the wave-vector modulus), it is possible to reconstruct fluctuations over the full spectrum, or, by selectively summing over each mode (for example, if $c^n \tau / |d^n| > L^\Delta$), to reconstruct only that portion of the spectrum which corresponds to resolvable structures. In hybrid RANS/LES, small-scale fluctuations are represented by the SGS model, and therefore the synthetic reconstruction is limited to wavelengths larger than that of the Nyquist grid scale. Thus, no summation is made for mode n (its associated trigonometric functions are simply not evaluated) if the modal wavelength is unresolvable. As a result of the required filtering, the cost of these additional trigonometric functions is negligible everywhere other than at interface regions. The additional storage requirements for this synthetic reconstruction relate only to the number of modes and are independent of the grid size.

The energy extracted from this stochastic model of turbulence can be determined analytically from the energy distribution used to produce the initial sampling. Alternatively, this can be determined numerically, by summing the contribution from each mode. For example, by integrating over a sufficiently long period of time one can obtain the following energy fraction for mode n :

$$\frac{k(n)}{k} = \frac{\left[(p_i^n)^2 + (q_i^n)^2 \right]}{\sum_{m=1}^N \left[(p_i^m)^2 + (q_i^m)^2 \right]} \quad (15)$$

This theoretical fraction of energy drained from k is strictly correct only over a long time-integration period. In practice, the data transfer is an instantaneous process, carried out in an operator splitting fashion prior to each time-integration step. Thus, in reality, the transfer period is never sufficiently long to guarantee that the preceding theoretical fraction is reached. However, if there is a constant source of statistical turbulence energy (fed in through convective or diffusive transport) the extracted energy fraction will be correct on the average.

It needs to be acknowledged that the reconstructed energy fraction can differ from the $(1 - \alpha)k$ fraction determined by the LNS method. Currently both fractions are used independently. The LNS latency parameter is derived from a constraint that the shear-stress blend continuously between that prescribed by the underlying turbulence model and that of the underlying subgrid closure. Alternative partitions can, of course, be derived using other modeling assumptions or alternative RANS/LES models.

IV. Application to Fully Developed Channel Flow

The case of plane channel flow is considered with periodic spanwise and streamwise boundary conditions and a mean pressure gradient imposed in the streamwise direction. All cases presented used the LNS method with the large-scale energy transfer. This energy-transfer process is denoted Large-Eddy STimulation (LEST). The first case presented is that of a Re_τ (Reynolds number based on friction velocity) equal to 2×10^3 . The mesh consisted of 64 (streamwise) \times 64 (normal to wall) \times 32 (spanwise) points and covered a domain of $2\pi \times 2 \times \pi$. Clustering was imposed in the normal-to-wall direction to ensure that y^+ was approximately $\frac{1}{2}$. In hybrid RANS/LES, y^+ again takes its traditional meaning as a local Reynolds number based on the friction velocity and distance Δy from the wall to the centroid of the first off-wall cell:

$$y^+ = u_\tau \Delta y / \nu \quad (16)$$

The calculation was started from an analytic profile for the steady mean velocity and turbulence energy, with the large-scale energy transfer immediately generating velocity fluctuations from these imposed conditions.

Numerical details were found to be much more important for this case than for previously computed high-Reynolds-number separated flows.^{3,4} A condition of Courant–Friedrichs–Lewy ($|u_i| < 1$) was enforced in all cells away from the RANS layer and second-order time stepping was used throughout, with residuals from the inner, subiterations converged at least one order of magnitude at each time step. Any form of upwinding was found to quickly dissipate the resolved-scale structures, and therefore a 95% blend of central differencing was used for the momentum equations. (Full second-order upwinding was retained only for the transported turbulence variables.)

Time averages were taken over approximately 20 flow-through times. Figure 2 shows the total shear stress and its corresponding contributions from the unresolved (modeled) and directly resolved components. There is a curious tendency to create a very small inflection in the shear stress, which persists even after very many flow-through times (even though this should be linear once it balances the streamwise pressure gradient). Similar channel-flow calculations have been produced previously by Nikitin et al.,¹⁸ using the basic DES model of Spalart et al.² The significance of the present calculations is that, for the first time, these simulations include a continuous and automatic conversion of energy between the RANS and LES data representations.

Figures 3 and 4 show the shear-stress and mean velocity profiles computed on a coarser mesh at $Re_\tau = 395$. Comparisons are shown against the (unpublished) DNS work of Kim (1989). The normal-to-wall resolution was, again, set to 64 points, with $y^+ < 1$, but the mesh spacing in the remaining directions was significantly coarsened, leaving only 14 points in the streamwise direction and only 7 points in the span.

At this extremely low resolution, the resolved-scale fluctuations were quickly dissipated without the large-scale energy transfer. This

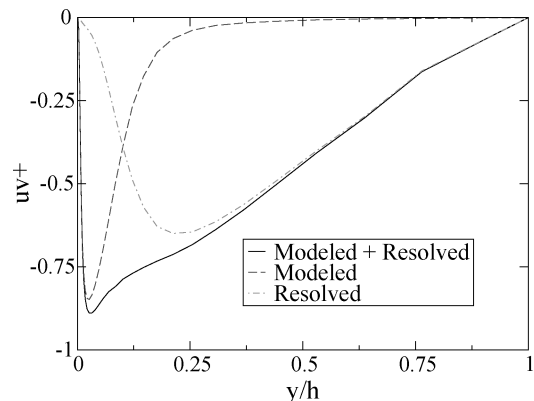


Fig. 2 Shear-stress profile from channel flow ($64 \times 64 \times 32$) at $Re_\tau = 2 \times 10^3$: LNS + LEST.

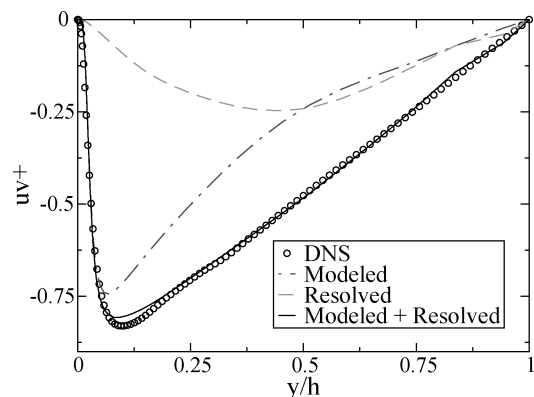


Fig. 3 Shear-stress profile from channel flow ($14 \times 64 \times 7$) at $Re_\tau = 395$: LNS + LEST.

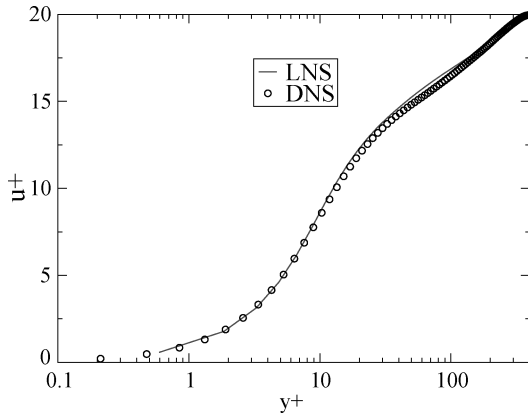


Fig. 4 Mean velocity profile from channel flow ($14 \times 64 \times 7$) at $Re_\tau = 395$: LNS + LEST.

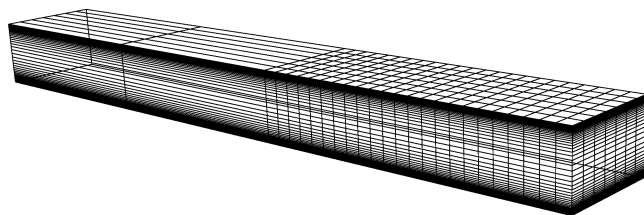


Fig. 5 Channel-flow grid showing streamwise clustering.

problem was referred to earlier as a component laminarization (in this case, a laminarization of the resolved-scale turbulence). In the absence of any large-scale energy transfer, the difficulty that must be anticipated is the quasi-steady boundary condition that the inner (core) region of the channel flow will experience as a result of the near-wall RANS layer. If the majority of the boundary layer is treated with RANS, the remaining (resolved) kinetic energy can simply become too weak to sustain itself, particularly in the presence of the larger effective viscosity resulting from the RANS layer. This situation leads to an underestimation of the total shear stress and hence an incorrectly predicted mean velocity profile. This example shows that the large-scale energy transfer is able to help sustain even very coarse-mesh simulations of unsteady boundary layer flow.

V. Channel Flow with Streamwise Clustering

A channel flow at $Re_\tau = 395$ is next considered, with a grid of 25 (streamwise) \times 74 (normal to wall) \times 7 (spanwise) mesh points covering a domain of $[-3\pi, 4\pi] \times [0, 2] \times [0, \pi]$. Upstream, the grid is heavily elongated to force RANS-like behavior in the first two rows of cells. At $x = \pi$, the mesh is abruptly clustered in the streamwise direction (Fig. 5). The subsequent streamwise spacing then roughly matches that in the span and allows some of the larger-scale turbulent flow structures to be directly resolved. The large-scale energy transfer procedure immediately converts the larger wavelength modes of the turbulence energy away from the channel wall into fluctuations in the resolved velocity components.

Figure 6 illustrates the development of the streamwise vorticity (shaded with the streamwise velocity component), showing the initiation of the resolved scales of motion downstream of the clustering at $x = \pi$.

Time- and span-averaged probes were placed at locations $3h$, $4h$, $5h$, $6h$, $8h$, and $10h$ in the streamwise direction. Figures 7–12 show the total and component shear stresses at each of these streamwise locations. Figure 7 shows the rake placed in the row of cells just prior to the clustering—a row in which cells were still stretched in the streamwise direction to enforce RANS behavior. The rake shows no resolved stress contribution and only a very mild distortion in response to the unsteady field downstream. Figure 8 shows the results of the first rake downstream of the abrupt clustering. The modeled shear-stress component is now suppressed toward the

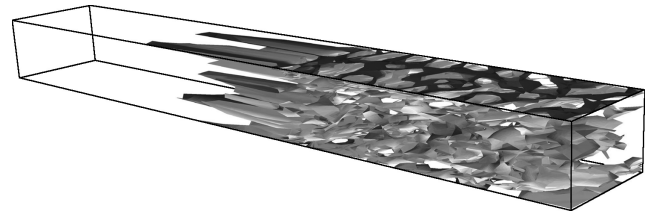


Fig. 6 Instantaneous streamwise vorticity isosurfaces shaded with the streamwise velocity component.

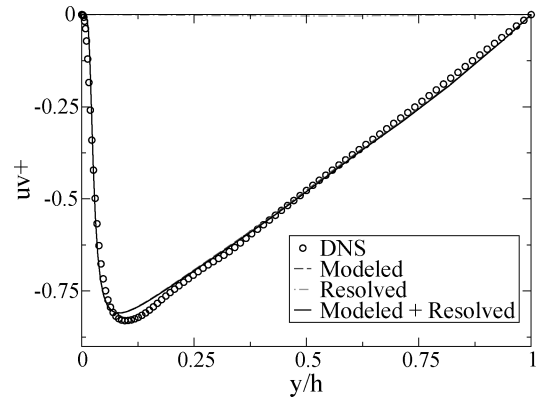


Fig. 7 Shear-stress profiles at $x = 3h$.

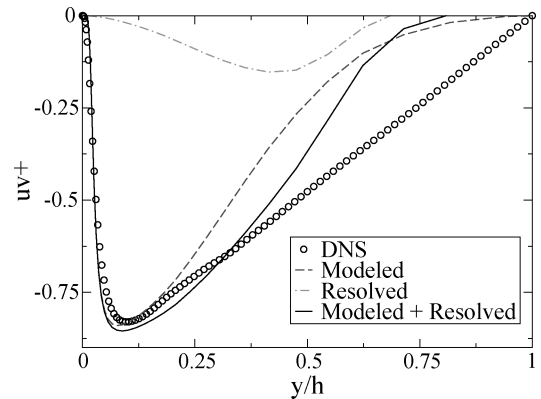


Fig. 8 Shear-stress profiles at $x = 4h$.

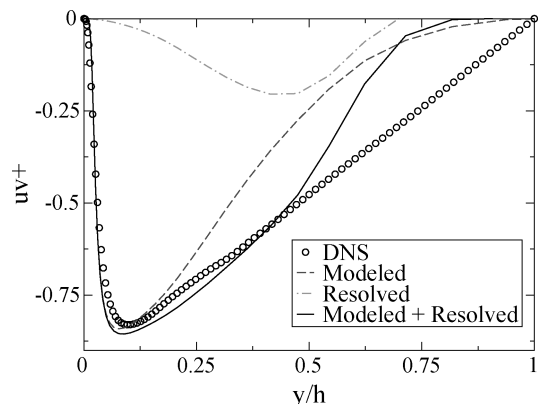


Fig. 9 Shear-stress profiles at $x = 5h$.

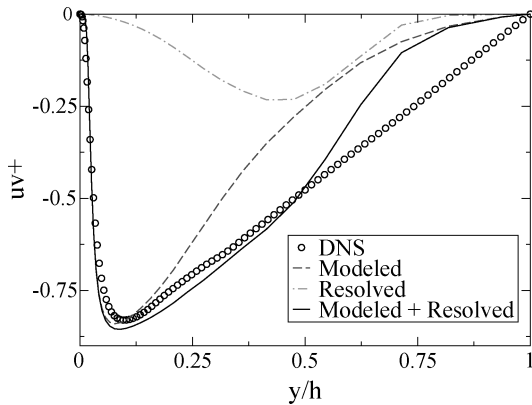


Fig. 10 Shear-stress profiles at $x = 6h$.

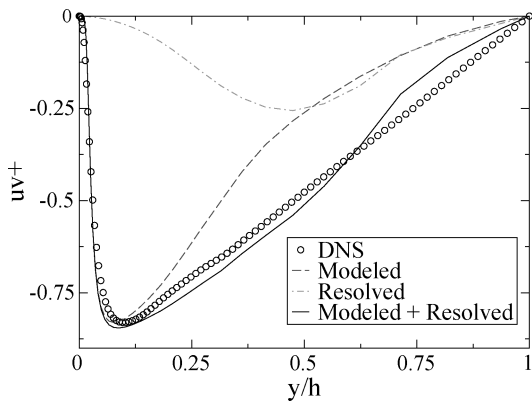


Fig. 11 Shear-stress profiles at $x = 8h$.

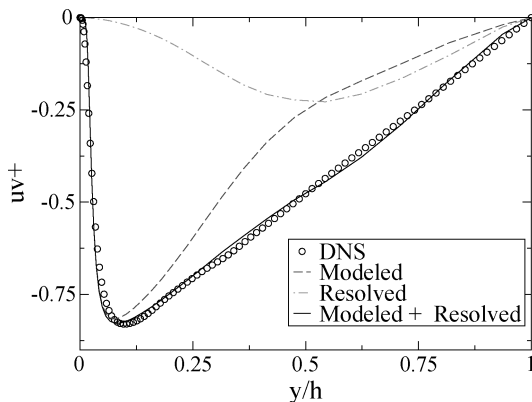


Fig. 12 Shear-stress profiles at $x = 10h$.

channel centerline, but the resolved component is not sufficiently well developed in that location. It is possible that disturbances in the mean-strain field prevent a more rapid translation of the anisotropy into resolved velocity components because of a constantly shifting target Reynolds-stress tensor. Farther downstream, at locations $5h$, $6h$, $8h$, and $10h$ (Figs. 9–12) the resolved (and hence total) stress profiles improve slowly. (In the absence of the large-scale energy transfer, no resolved shear stress is recovered.)

VI. Summary

This paper has considered extending the applicable range of hybrid RANS/LES models to include an automatic initiation of LES fluctuations as RANS data are transported from coarse-mesh into fine-mesh regions. This work was motivated by the neglect, in all current hybrid RANS/LES variants, of the transfer between statistically modeled and directly resolved components of the turbulence kinetic energy, a transfer that should occur at any interface or region

in which the model equations switch (either gradually or abruptly) from RANS to LES.

The energy transfer procedure also removes any need for the user to impose unsteady initial conditions because any large-scale (statistical) kinetic energy imposed will be automatically converted into velocity fluctuations prior to the first integration step of the solver. Because of the required filtering employed, the cost associated with the trigonometric function evaluations is negligible everywhere other than at interface regions.

This paper has specifically considered the interfaces created by a downstream clustering, into which statistically represented turbulence is convected, and the interfaces across a boundary layer, where statistically represented energy is transported through turbulent motions from the near-wall RANS layer into the outer LES region. Energy transfer into the resolved-scales automatically provides appropriate inlet boundary conditions to embedded LES regions and, at the coarser grid resolutions intended with hybrid RANS/LES, helps maintain the unsteady motion within the resolved portion of the boundary layer. The suggested procedure creates a synthetic field of velocity fluctuations, which over a long time average achieves the target second moments, timescales, and lengthscales from a given set of RANS statistics. The procedure requires no additional transport equations and only minimal additional storage. As input, it requires a dissipation rate and a realizable set of Reynolds-stresses. This information is directly available within the LNS model.

It should be emphasized that much of the presented material is work in progress. The transfer from RANS to LES data does require some transient period. It is likely that improvements can be made to the synthetic turbulence model; however, even very accurate unsteady inlet data would still require some transient period for the solution to adjust to the new spatial and temporal resolution of the given mesh and numerics. The situation is, of course, likely to be worse for synthetic methods because there will be many properties of the Navier–Stokes equations (in fact, an infinite number) that are not satisfied by the synthetic reconstruction. There is also a question of how the induced fluctuations are being damped by the (possibly large) values of eddy viscosity in the remaining near-wall portion of the boundary layer. Additionally, high-speed flows will require further models for temperature and density fluctuations.

References

- Speziale, C. G., "Computing Non-Equilibrium Flows with Time-Dependent RANS and VLES," *15th ICNMF*, Lecture Notes in Physics, Springer-Verlag, 1996.
- Spalart, P. R., Jou, W.-H., Strelets, M., and Allmaras, S., "Comments on the Feasibility of LES for Wings and on a Hybrid RANS/LES Approach," *Advances in DNS/LES*, edited by C. Liu and Z. Liu, Greyden Press, Columbus, OH, 1997.
- Batten, P., Goldberg, U. C., and Chakravarthy, S. R., "Sub-Grid Turbulence Modeling for Unsteady Flow with Acoustic Resonance," AIAA Paper 00-0473, Jan. 2000.
- Batten, P., Goldberg, U., and Chakravarthy, S., "LNS—An Approach Towards Embedded LES," AIAA Paper 2002-0427, Jan. 2002.
- Batten, P., Goldberg, U., and Chakravarthy, S., "Using Synthetic Turbulence to Interface RANS and LES," AIAA Paper 2003-0081, Jan. 2003.
- Strelets, M., "Detached Eddy Simulation of Massively Separated Flows," AIAA Paper 2001-0879, Jan. 2001.
- Arunajatesan, S., and Sinha, N., "Unified Unsteady RANS-LES Simulations of Cavity Flowfields," AIAA Paper 2001-0516, Jan. 2001.
- Fan, T. C., Xiao, X., Edwards, J. R., Hassan, H. A., and Baurle, R. A., "Hybrid LES/RANS Simulation of a Mach 3 Shock Wave/Boundary Layer Interaction," AIAA Paper 2003-0080, Jan. 2003.
- Menter, F. R., Kuntz, M., and Bender, R., "A Scale-Adaptive Simulation Model for Turbulent Flow Predictions," AIAA Paper 2003-0767, Jan. 2003.
- Travin, A., Shur, M., Strelets, M., and Spalart, P. R., "Detached-Eddy Simulations past a Circular Cylinder," *Flow, Turbulence and Combustion*, Vol. 63, 2000, pp. 293–313.
- Forsythe, J., Hoffman, K., and Squires, K. D., "Detached-Eddy Simulation with Compressibility Corrections Applied to a Supersonic Axisymmetric Base Flow," AIAA Paper 2002-0586, Jan. 2002.
- Kraichnan, R. H., "Diffusion by a Random Velocity Field," *Physics of Fluids*, Vol. 13, No. 1, 1969, pp. 22–31.
- Smirnov, A., Shi, S., and Celik, I., "Random Flow Generation Technique for Large Eddy Simulations and Particle-Dynamics Modeling," *Journal of Fluids Engineering*, Vol. 123, 2001, pp. 359–371.

¹⁴Smagorinsky, J., "General Circulation Experiments with the Primitive Equations," *Monthly Weather Review*, Vol. 91, 1963, pp. 99–165.

¹⁵Goldberg, U., Batten, P., Palaniswamy, S., Chakravarthy, S., and Peroomian, O., "Hypersonic Flow Predictions Using Linear and Nonlinear Turbulence Closures," *Journal of Aircraft*, Vol. 37, No. 4, 2000, pp. 671–675.

¹⁶Hanjalic, K., Launder, B. E., and Schiestel, R., "Multiple Time-Scale Concept in Turbulent Transport Modelling," *Turbulent Shear Flows II*, Springer-Verlag, 1980.

¹⁷Schiestel, R., "Multiple-Scale Concept in Turbulence Modelling, II Reynolds Stresses and Turbulent Heat Fluxes of a Passive Scalar, Algebraic Modelling and Simplified Model Using Boussinesq Hypothesis," *Journal of Mechanical Theory and Applications*, Vol. 2, 1983, pp. 601–615.

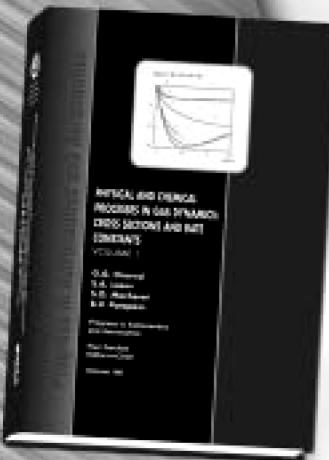
¹⁸Nikitin, N. V., Nicoud, F., Wasistho, B., Squires, K. D., and Spalart,

P. R., "An Approach to Wall Modeling in Large-Eddy Simulations," *Physics of Fluids*, Vol. 12, No. 7, 2000, pp. 1629–1632.

¹⁹Baggett, J. S., "On the Feasibility of Merging LES with RANS for the near-Wall Region of Attached Turbulent Flows," CTR Annual Research Briefs, Technical Rept., Center for Turbulence Research, Stanford Univ., Stanford, CA, 1998.

²⁰Peltier, L. J., and Zajackowski, F. J., "Maintenance of the near-Wall Cycle of Turbulence for Hybrid RANS/LES of Fully-Developed Channel Flow," *Proceedings of the Third AFOSR International Conference on DNS/LES*, edited by C. Liu, L. Sakell, and T. Beutner, Greyden Press, 2001.

F. Grinstein
Guest Editor



Progress in Astronautics and Aeronautics Series
2002, 311 pp, Hardback with Software
ISBN: 1-56347-518-9
List Price: \$90.95
AIAA Member Price: \$64.95

Physical and Chemical Processes in Gas Dynamics: Cross Sections and Rate Constants, Volume I


**G. G. Chernyi and S. A. Losev, Moscow State University,
S. O. Macheret, Princeton University, and B. V. Potapkin, Kurchatov Institute,
Editors**

Contents:

- General Notions and Essential Quantities
- Elastic Collisions in Gases and Plasma (T-Models)
- Rotational Energy Exchange (R Models)
- Vibrational Energy Exchange (V Models)
- Electronic Energy Exchange (E Models)
- Chemical Reactions (C Models)
- Plasma Chemical Reactions (P Models)

This unique book and accompanying software CARAT provide concise, exhaustive, and clear descriptions of terms, notations, concepts, methods, laws, and techniques that are necessary for engineers and researchers dealing with physical and chemical process in gas and plasma dynamics. This first volume of a multi-volume set covers the dynamics of elementary processes (cross sections and rate coefficients of chemical reactions, ionization and recombination processes, and inter- and intramolecular energy transfer).

The text and Windows-based computer program CARAT—toolkit from Chemical Workbench model library—carry widely diversified numerical information about 87 models for collision processes in gases and plasmas with participation of atoms, molecules, ions, and electrons. The processes include elastic scattering, electronic-vibration-rotation energy transfer between colliding molecules, chemical and plasma-chemical reactions. The databases of recommended particle properties and quantitative characteristics of collision processes are built in. Computer implementation of models allows one to calculate cross sections for elastic and inelastic collisions, and rate constants for energy transfer processes and reactions within a wide range of parameters and variables, i.e., the collision energy, gas temperature, etc. Estimates of the accuracy of cross sections and rate coefficient represent an important part of the description of each model.



American Institute of Aeronautics and Astronautics

American Institute of Aeronautics and Astronautics, Publications Customer Service, P.O. Box 960, Herndon, VA 20172-0960
Fax: 703/661-1501 • Phone: 800/682-2422 • E-mail: warehouse@aiaa.org • Order 24 hours a day at www.aiaa.org

02-0554